Journal of Asian Earth Sciences 276 (2024) 106354

Contents lists available at ScienceDirect

Journal of Asian Earth Sciences

journal homepage: www.elsevier.com/locate/jseaes

Explicit role of seamount subduction in upper plate deformation as exemplified in the Ryukyu subduction zone

Xiaobo He *, Qin Zhou

Marine Science & Technology College, Zhejiang Ocean University, Zhoushan, Zhejiang 316022, China

ARTICLE INFO

Keywords:
Ryukyu subduction zone
Seamount subduction
Subduction erosion
Back-arc rifting
Outer rise bending
Forearc extension

ABSTRACT

The Ryukyu subduction zone is typical of the subduction of an oceanic ridge (seamount or plateau) and back-arc rifting. How the upper plate responds to the combined effect of subduction of a bathymetric high and back-arc spreading is not fully understood. We investigate the combined effect by calculating the T-axis from regional focal mechanisms. Three patterns are observed from the outer rise to the back arc, showing a coherent trench-normal T-axis along the strike. They can be readily explained by outer-rise plate bending, forearc upper-plate bending induced by seamount subduction, and back-arc spreading associated with slab rollback. A distinct pattern of trench-parallel T-axes along the strike is also observed in the arc. This can be attributed to the difference in the extension rate between forearc extension and back-arc rifting of the upper plate, where the rate of back-arc extension driven by slab rollback is faster than that of forearc trench-normal extension attributed to seamount subduction. We also examine the T-axis patterns in other systems with seamount subduction, including the southern Manila subduction zone and the southern Central to northern South American subduction zones, displaying similar trench-normal T-axes in the forearc. Therefore, our observations have a broader implication in upper-plate deformation in response to seamount subduction.

1. Introduction

The NE-trending Ryukyu subduction system extends ~ 1,000 km from the southwest of Kyushu, Japan, to the east of Taiwan. It results from the Philippine Sea plate (PSP) subduction beneath the Eurasian plate (Fig. 1). Several key tectonic components uniquely characterize this system, including (1) an active back-arc basin of the Okinawa Trough (OT) with a rifting rate that progressively increases from ~ 23 mm/yr in the north to ~ 46 mm/yr in the south (Arai et al., 2017), (2) intraplate seismicity with a focal depth of 150–300 km (Jia and Sun, 2021), (3) bathymetric anomalies (the Gauga Ridge, the Daito Ridge, and the Amami Plateau) interacting with the Ryukyu Trench (He et al., 2022; Wang et al., 2022).

It has long been recognized that subduction of a bathymetric high, such as a fossil oceanic ridge, oceanic plateau, or seamount, affects various tectonic processes at a subduction zone (e.g., Dominguez et al., 2000; Wang and Bilek, 2011; Morgan and Bangs, 2017; Tao et al., 2020; Liu, 2021; Pajang et al., 2022; Passarelli et al., 2022; Yan et al., 2022). More specifically, it affects (1) plate hydration and arc magmatism (e.g., Kim and Clayton, 2015; Jang et al., 2019; He et al., 2022; Pan and He, 2023), (2) slab dip angle (e.g., Liu et al., 2008; Zhao and Leng, 2023), (3) subduction erosion (e.g., Dominguez et al., 2000; Bangs et al., 2006; Straub et al., 2020), (4) interplate coupling and seismic rupture (e.g., Scholz and Small, 1997; Sun et al., 2020; Wang and Lin, 2022; Gase et al., 2023), (5) slab break-off timing (e.g., Cheng et al., 2019), (6) intraplate seismicity (e.g., Zhang et al., 2021), (7) upper plate fracturing (e.g., Prada et al., 2023), (8) accretionary wedge deformation (e.g., Ruh et al., 2016; Wang et al., 2019; Wang et al., 2021; Miyakawa et al., 2022), (9) forearc drainage system (e.g., Zeumann and Hampel, 2017), and (10) coastal uplift (e.g., Pedoja et al., 2006).

The Ryukyu subduction zone is a typical setting with more than one bathymetric high at the trench (Fig. 1), where from west to east, the Gagua Ridge (e.g., Wang et al., 2022), the Daito Ridge and the Amami Plateau interact with the trench (e.g., He et al., 2022). In addition, this subduction zone has perhaps experienced back-arc rifting at the Okinawa Trough since the early Pleistocene (e.g., Kimura, 1985; Minami et al., 2022). It is well known that the arrival of a bathymetric high at the trench prevents the trench retreat (e.g., Zhao and Leng, 2023), a vital process for maintaining back-arc opening (Sdrolias and Müller, 2006). The coexistence of oceanic plateaus at the trench and active back-arc

* Corresponding author.
E-mail address: xiaobo.he@zjou.edu.cn (X. He).

https://doi.org/10.1016/j.jseaes.2024.106354
Received 24 October 2023; Received in revised form 11 September 2024; Accepted 1 October 2024
Available online 2 October 2024

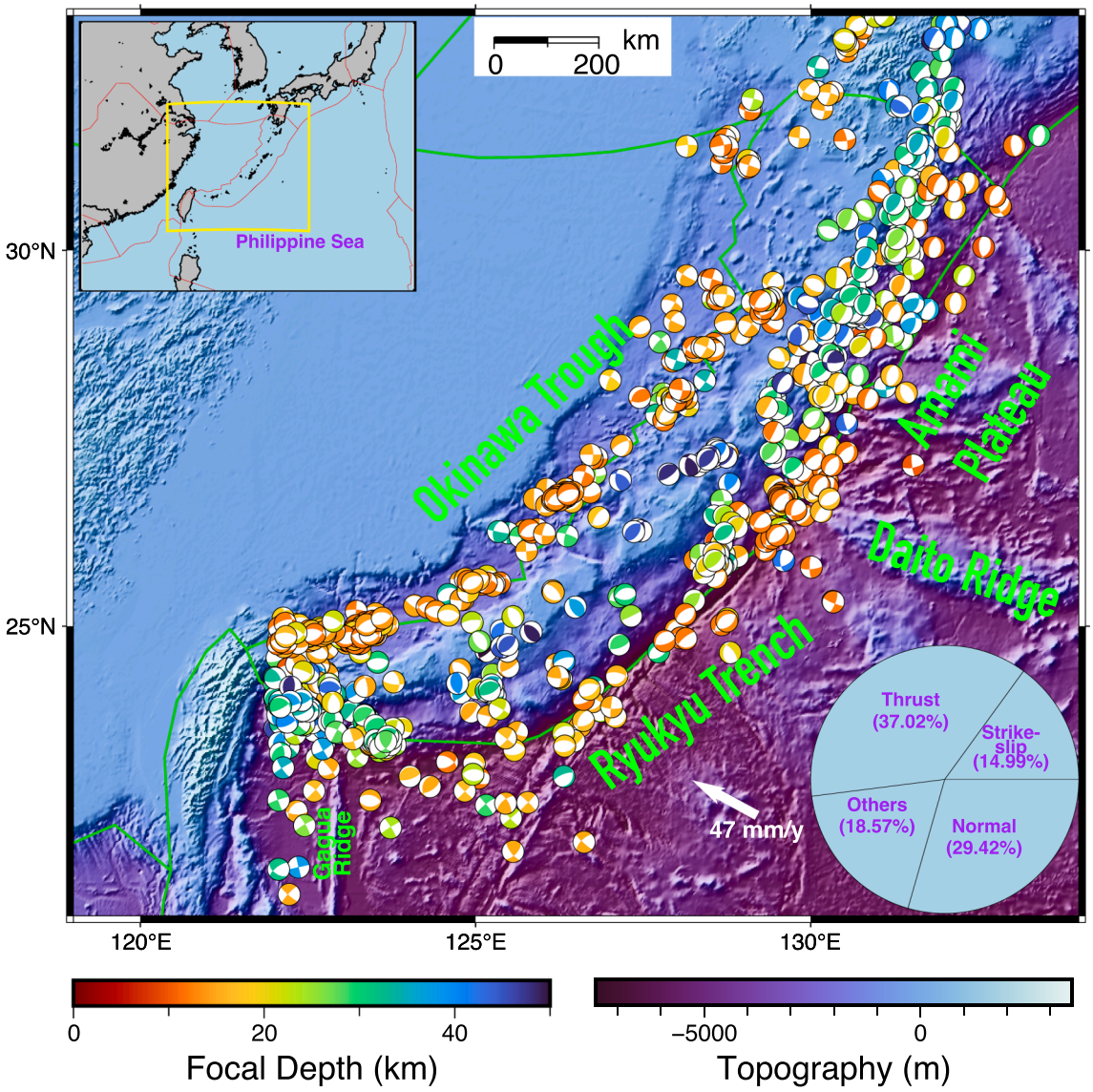

Fig. 1. Tectonic map of the Ryukyu subduction zone showing M > 4.5 earthquakes with focal depths less than 50 km occurred from Jan. 1, 1976, to Jan. 1, 2023, exhibited by focal mechanisms (beachballs), which is characterized by subduction of Gagua Ridge, Daigo Ridge, and Amami Plateau and back-arc rifting in the Okinawa Trough. The bottom right insert (Pie chart) shows the event type classification of earthquakes. The arrow indicates the absolute plate motion of the Philippine Sea plate given by the No-Net-Rotation model of NNR-MORVEL56 (Argus et al., 2011). The plate boundary data, depicted with red (in the upper left insert) and green lines, are given by the PB2002 model (Bird, 2003).

rifting thus makes this subduction zone a unique setting for understanding how different competing factors influence upper plate deformation, which is intriguing but has not been addressed.

A subduction setting is abundant in thrust-fault earthquakes due to two plates' convergence, but occasionally, normal-fault earthquakes occur. What processes are responsible for normal-fault earthquakes? This study calculates the T-axis (Tension axis) to examine the upper plate's deformation patterns, which directly reflect extensional stress based on regional focal mechanisms. We discuss how the upper plate responds to the combined effect of the subduction of multiple bathymetric anomalies at the trench and the back-arc spreading. We also examine the T-axis patterns in other subduction systems with the subduction of a bathymetric high, including the southern Manila subduction zone and the southern Central to northern South American subduction zones, to characterize the behavior of upper-plate extension under similar tectonic environments.

2. Data and analysis

From the global CMT catalog (Dziewoński et al., 1981; Ekström et al., 2012), we collect the focal mechanisms for the regional M > 4.5 earthquakes with focal depths less than 50 km from 1 January 1976 to 1 January 2023. Fig. 1 shows the plotted focal mechanisms in colored beachballs and event-type classification of the earthquakes in a pie chart, with normal-fault earthquakes accounting for nearly 30 % of the total events. We followed our previous scheme applied to the Japanese subduction zone (Choi et al., 2012). It is similar to the procedure introduced by Gasperinia and Vannuccib (2003). Specifically, the directions of extensional stress axes (T-axes) are calculated from the fault-plane solutions and slip vectors. The T-axis unit vector, $\hat{t}$, is given by (Aki and Richards, 1980)

$$\hat{t} = \frac{\hat{n} + \hat{d}}{\sqrt{2}} \tag{1}$$

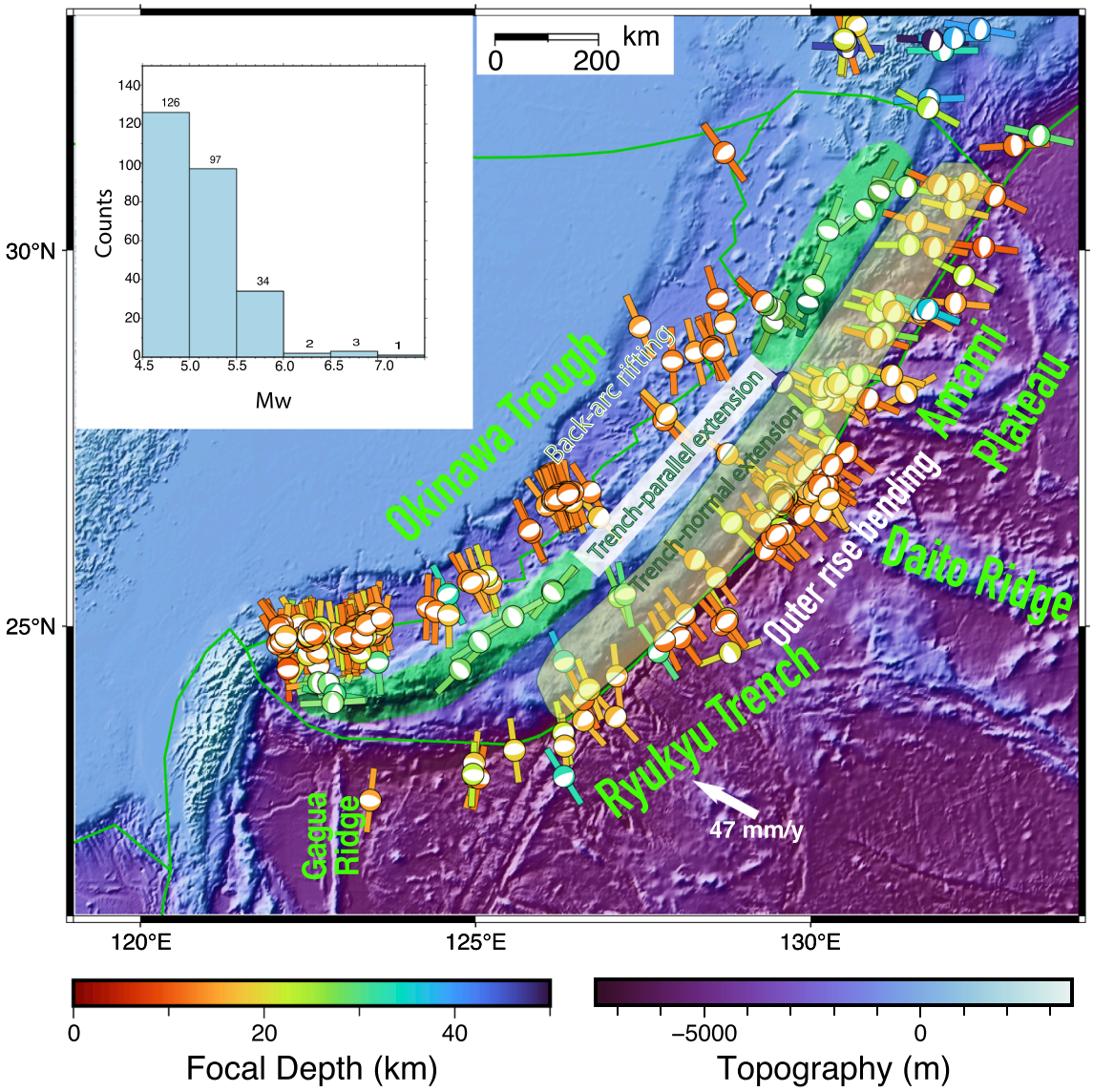

Fig. 2. Tectonic map of the Ryukyu subduction zone showing normal fault earthquakes (beach balls) and calculated T-axes (short bars). The upper left insert shows histograms of the event magnitude distribution of normal fault earthquakes. The green shadow indicates the zone subjected to trench-parallel extension. The purple shadow indicates the zone subjected to trench-normal extension induced by subduction erosion. The back-arc trench-normal extension occurs in the Okinawa Trough.

where $\hat{n}$ is the unit normal vector of the fault plane, and $\hat{d}$ is the unit slip vector. Note that the P and T axes are at angles of 45° with the nodal planes.

The T-axis calculations in this study are restricted to normal-fault earthquakes. The calculated results are shown in Fig. 2.

3. Results and discussion

Trench-normal or trench-parallel T-axes along the strike are observed in this subduction zone. Specifically, three belts along the strike have trench-normal T-axes, and one belt has trench-parallel T-axes. Three trench-parallel T-axis belts are distributed in the outer rise, forearc, and back-arc regions, while one trench-parallel T-axis belt coincides spatially with the arc region (Fig. 2).

3.1. Trench-normal T-axis in the outer rise

The trench-normal T-axis in the outer rise can be readily explained by the bending of the descending PSP, which leads to trench-normal extensional stress. This scenario has been well-studied observationally (e.g., Levitt and Sandwell, 1995; Mark et al., 2023) and numerically (e.g., Zhou et al., 2015; Yang et al., 2022) in different subduction zones. The outer rise bending also contributes to plate hydration, which carries water flux into the mantle (Pan and He, 2023).

3.2. Trench-normal T-axis in the forearc

The trench-normal T-axes in the forearc can be explained by upper plate flexure driven by seamount subduction, a tectonic process that leads to normal faulting in the upper plate and is closely associated with seamount subduction (Clift et al., 2003; von Huene et al., 2004; Straub et al., 2020). This process plays an important role in removing upper-plate material from the forearc at convergent margins, which transfer a significant amount of crustal material into the Earth's mantle at subduction zones; in particular, seamount subduction favors tectonic erosion of the frontal margin (e.g., Dominguez et al., 2000).

Upper-plate bending in the forearc is particularly favored by seamount subduction because the arrival of seamounts at the trench significantly increases the interplate coupling (e.g., Sun et al., 2020) and uplifts the upper plate (Prada et al., 2023). It thereby increases the

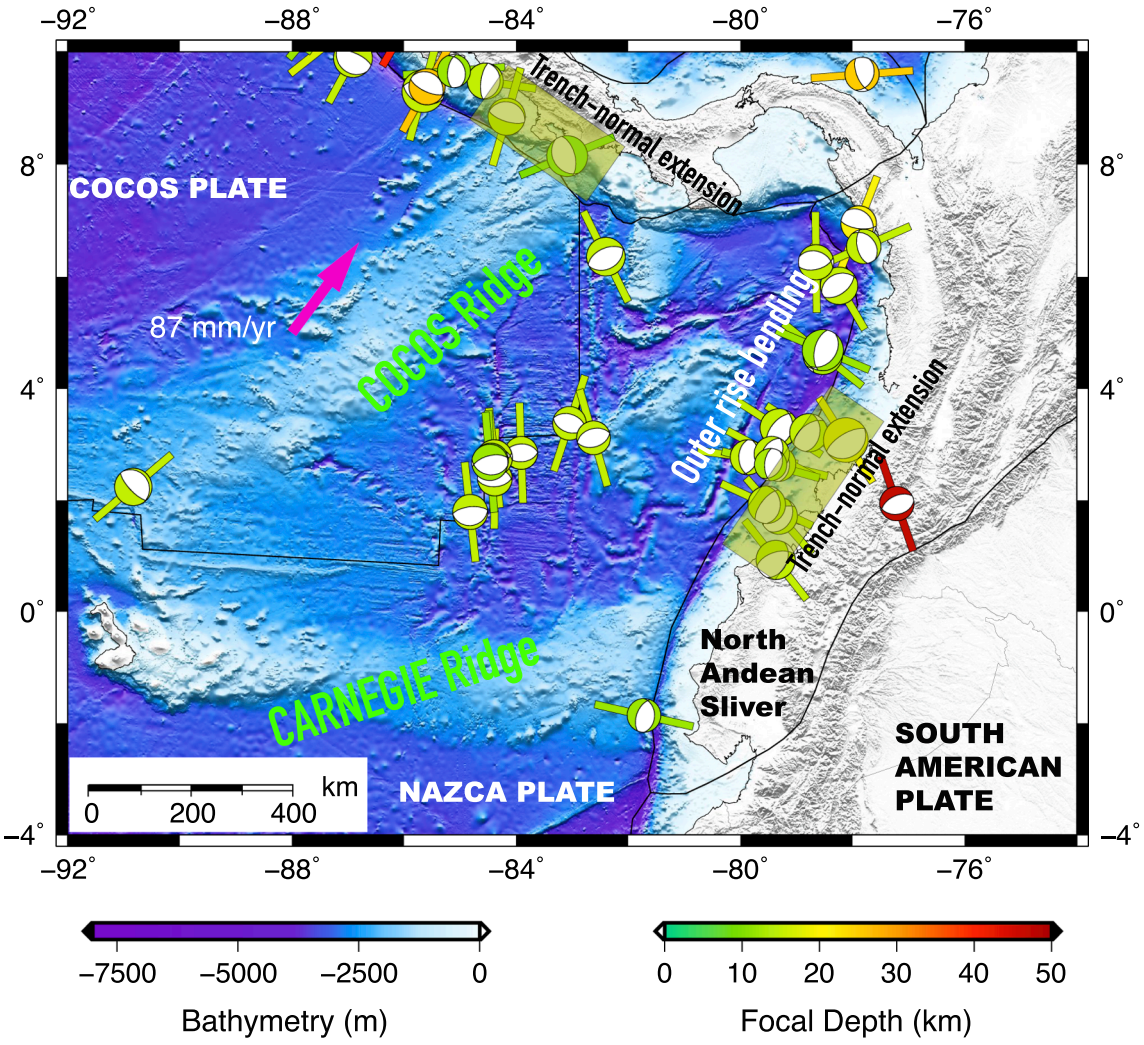

Fig. 3. Tectonic map of the southern Central American subduction zone and northern South American subduction zone, showing normal fault earthquakes (beach balls) and calculated T-axes (short bars), where the Cocos Ridge and Carnegie Ridge meet the trenches. Trench-normal T-axes (green shadows), indicating trench-normal extensions, are observed at the forearc in response to the arrival of the ridges at the trenches.

forearc slope angle up to ~ 5.2° in the Ryukyu subduction zone (Clift and Vannucchi, 2004), a value larger than the 1.5° to 2.5° values mainly found in the accretionary margins (Clift and Vannucchi, 2004). The materials in the upper plate, particularly the frontal prism, can be passively dragged down into subduction channels by the descending slab, resulting in an extensional upper plate and normal faults (von Huene et al., 2004). Therefore, trench-normal extensional stress can develop in the forearc as seamount subduction occurs, consistent with the trench-normal T-axes observed along the strike.

Upper-plate bending in the forearc is particularly favorable in the Ryukyu subduction zone because three bathymetric anomalies interact with the trench from west to east. This results in an intensely stretched upper plate, as evidenced by the wide distribution of normal-fault earthquakes in the forearc (Fig. 2). A recent study suggests that subducting ridges uplift the margin, causing upper plate fractures and areas of low rigidity (Prada et al., 2023). Moreover, fluids from the subducted plate flow into the upper plate, penetrating extensional fractures (von Huene et al., 2004). All these consequences provide favorable conditions for upper plate deformation, especially forearc trench-normal extension accompanied by the descending slab.

3.3. Comparisons with other subduction systems

To further support our argument that trench-normal extension occurs in the erosional margins, we present a similar T-axis distribution map in the southern Central to northern South American subduction zones (Fig. 3) where subduction erosion has been recognized in the margins (Clift and Vannucchi, 2004) and is favored by ridge subduction such as the Cocos Ridge (e.g., Zeumann and Hampel, 2017) and Carnegie Ridge (e.g., Pedoja et al., 2006; Hernández et al., 2020; Margirier et al., 2023). As expected, trench-normal T-axes are observed along the strike in the margins, suggesting a similar stretching process in the upper plate associated with seamount subduction. We find no trench-parallel T-axes in the arc, which can be explained by the lack of back-arc spreading associated with slab rollback in the two subduction zones.

We also examine the T-axis distribution in the southern Manila subduction zone, where the convergence of two plates (i.e., the South China Sea plate and the PSP) occurs beneath Luzon and where the Zhenbei-Huangyan seamount chain in the south and a subducted oceanic plateau in the north meet the subduction zone, respectively (Fig. 4). As expected, trench-normal T-axes, associated with subduction of the seamount(s), are also observed along the strike in the margins. Interestingly, we observe trench-parallel T-axes along the strike near the arc. Unlike those in the Ryukyu subduction zone, which we attribute to the difference in extensional rate between two competing extensional processes, here we explain the trench-parallel T-axes as resulting from the interaction between two subductions (i.e., the southern Manila subduction and the east Luzon trough). The convergence of two

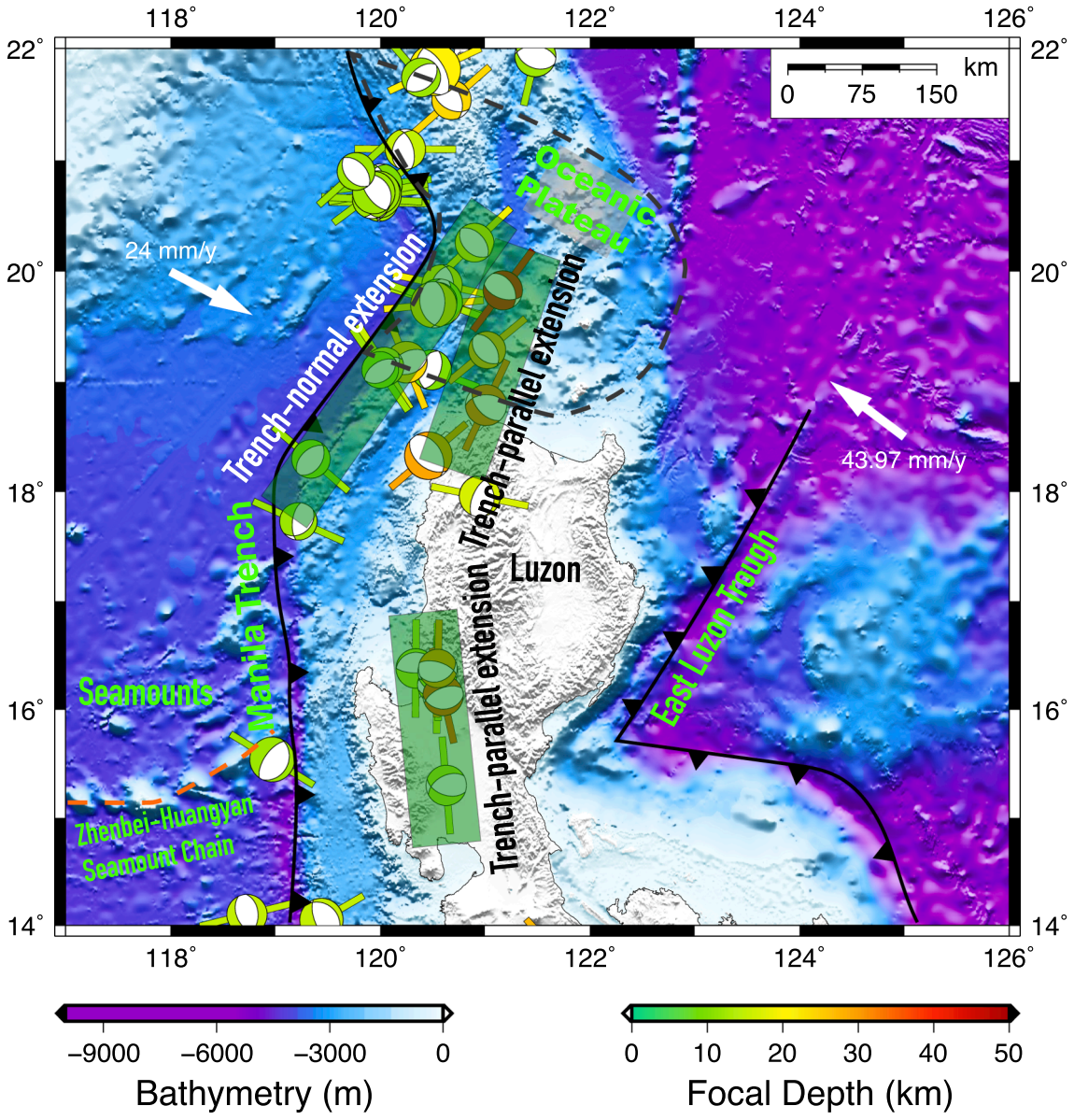

Fig. 4. Tectonic map of the southern Manila subduction zone, showing normal fault earthquakes (beach balls) and calculated T-axes (short bars), where the Zhenbei-Huangyan seamount chain (depicted with an orange dashed line) meets the trench in the south, and an oceanic plateau (depicted with a black dashed line) has long been recognized to subduct in the north (e.g., Ma et al., 2022).

subductions leads to trench-parallel extensions, as suggested by the trench-parallel T-axes (Fig. 4).

3.4. Rift axis-normal T-axis in the back-arc spreading center

The T-axes observed in the Okinawa Trough are consistently normal to the rift axis, indicating the active rifting process in the back-arc basin. Previous geophysical (e.g., Sato et al., 1994; Chen et al., 2018) and geochemical (e.g., Zeng et al., 2010) observations have also revealed the back-arc spreading operating in the Okinawa Trough. Thus, all lines of evidence point to a mature back-arc spreading in the Okinawa Trough, most likely driven by slab rollback and trench retreat.

3.5. Trench-parallel T-axis in the arc

The most intriguing tectonic signature is the trench-parallel T-axes along the strike observed in the arc. Although the number of normal-fault earthquakes exhibiting trench-parallel T-axes is small, they are coherently distributed along the strike in the arc (Fig. 2), suggesting a similar origin. As mentioned above, we attribute the trench-parallel extension to the difference in extensional rate between the back-arc rifting and forearc extension. It is proposed that a trench-normal compressional regime can develop if the back-arc spreading rate is faster than the extensional rate in the forearc. Such trench-normal compressional stress can readily generate trench-parallel extensional stress. This scenario is consistent with the trench-parallel T-axes observed along the strike in the arc. This trench-parallel extension plays a role in influencing the magmatic activity in the arc.

The different extensional rates in the upper plate can be estimated. More specifically, the orthogonal convergence rate in the Ryukyu subduction zone is ~ 70 mm/yr (Clift and Vannucchi, 2004), a value of the relative plate motion rate between the PSP and the upper Eurasian plate. The absolute plate motion of the PSP is ~ 47 mm/yr (Argus et al., 2011), leaving ~ 23 mm/yr for the upper plate. In contrast, the Okinawa Trough has an average half-spreading rate of ~ 12 mm/yr in the north to ~ 20 mm/yr in the south (Kimura, 1985; Arai et al., 2017). Thus,

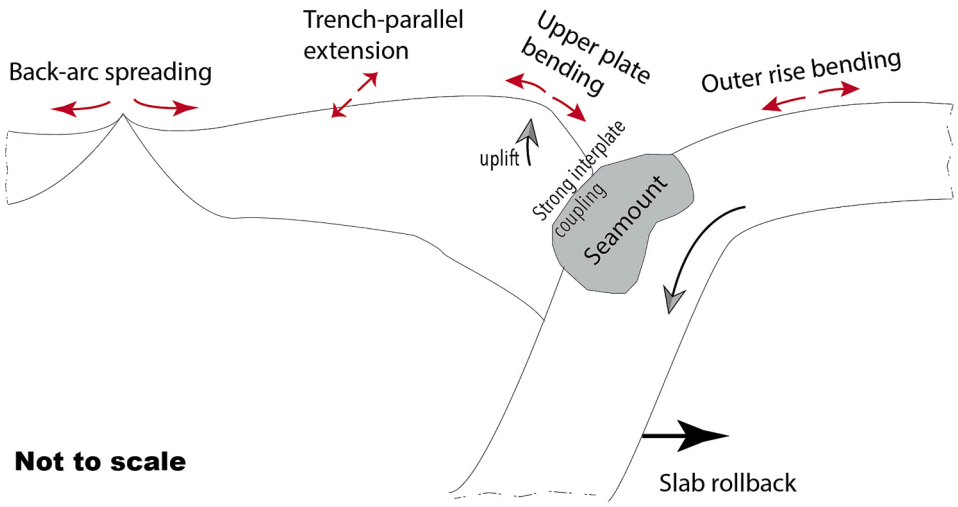

Fig. 5. Schematic illustration of the major tectonic components in a subduction zone characterized by seamount subduction and back-arc rifting, including back-arc spreading, trench-parallel extension, seamount subduction, and outer rise bending. Here, we use seamount to illustrate a bathymetric high. The divergent paired red arrows indicate extension directions, in which trench-normal extensions occur in the outer rise, forearc, and back-arc, whereas trench-parallel extensions appear in the arc. An arrow also indicates the slab rollback responsible for the back-arc spreading.

back-arc spreading has accommodated most of the trench-ward extension.

It is important to note that extensional forearc earthquakes can sometimes occur as aftershocks of large megathrust earthquakes (e.g., Klein et al., 2016). However, it cannot be applied to explain our observations for two reasons. First, the earthquake catalog employed in this study is not limited to aftershocks but includes all extensional earthquakes. Second, the subduction zone with seamount subduction is often not prone to megathrust earthquakes (e.g., Wang and Bilek, 2011; 2014), and the collected earthquakes are thus less likely to occur as aftershocks of large megathrust earthquakes.

Fig. 5 schematically illustrates the various tectonic processes leading to trench-normal or trench-parallel extension in this subduction zone. The conceptual model proposed in this study can be applied to other subduction zones with similar tectonic processes, especially those with seamount subduction and back-arc spreading.

4. Conclusions

Based on the calculated T-axes of normal-fault earthquakes, which mainly occurred in the upper plate in the Ryukyu subduction zone, this study shows how the upper plate stretches in response to the subduction of bathymetric highs and back-arc rifting. In particular, the trench-normal T-axes along the strike seen in the forearc can be attributed to upper-plate bending induced by oceanic plateau subduction. In contrast, the trench-parallel T-axes along the strike observed in the arc can be explained by the difference in strain rate driven by back-arc rifting and forearc trench-normal extension. The trench-normal T-axis is also observed in the outer rise along the trench axis, which the bending of the descending PSP can readily explain. Similar upper plate extension behaviors are found in other subduction zones with seamount subduction, such as the southern Manila subduction zone. The similarities across different subduction systems imply the broader implications of this study.

CRediT authorship contribution statement

Xiaobo He: Writing – review & editing, Writing – original draft, Supervision, Project administration, Methodology, Funding acquisition. **Qin Zhou:** Visualization, Investigation, Data curation.

Declaration of competing interest

The authors declare that they have no known competing financial interests or personal relationships that could have appeared to influence the work reported in this paper.

Data availability

No data was used for the research described in the article.

Acknowledgments

The figures were prepared with Generic Mapping Tools (Wessel and Smith, 1991). This work was funded by the National Natural Science Foundation of China (Grant Nos. 42076068, 42276049). The authors thank Juntao Tao for helping to make figures and Peter D. Clift for stimulating discussions. We are grateful for the constructive comments provided by the editor, the associate editor, and two anonymous reviewers, all of whom helped us considerably improve the manuscript.

References

Aki, K., Richards, P.G., 1980. Quantitative Seismology, Theory and Methods, Volume 1. W. H. Freeman and Company, San Francisco.

Arai, R., Kodaira, S., Yuka, K., Takahashi, T., Miura, S., Kaneda, Y., 2017. Crustal structure of the southern Okinawa Trough: Symmetrical rifting, submarine volcano, and potential mantle accretion in the continental back-arc basin. J. Geophys. Res. Solid Earth 122 (1), 622–641. https://doi.org/10.1002/2016jb013448.

Argus, D.F., Gordon, R.G., DeMets, C., 2011. Geologically current motion of 56 plates relative to the no-net rotation reference frame. Geochemistry, Geophysics, Geosystems 12. https://doi.org/10.1029/2011GC00375.

Bangs, N.L.B., Gulick, S.P.S., Shipley, T.H., 2006. Seamount subduction erosion in the Nankai Trough and its potential impact on the seismogenic zone. Geology 34 (8), 701–704. https://doi.org/10.1130/g22451.1.

Bird, P., 2003. An updated digital model of plate boundaries. Geochemistry Geophysics Geosystems 4 (3), 1027. https://doi.org/10.1029/2001GC000252.

Chen, H., Ikuta, R., Lin, C., Hsu, Y., Kohmi, T., Wang, C., et al., 2018. Back-Arc Opening in the Western End of the Okinawa Trough Revealed From GNSS/Acoustic Measurements. Geophys. Res. Lett. 45 (1), 137–145. https://doi.org/10.1002/2017gl075724.

Cheng, Z., Ding, W., Faccenda, M., Li, J., Lin, X., Ma, L., et al., 2019. Geodynamic effects of subducted seamount at the Manila Trench: Insights from numerical modeling. Tectonophysics 764, 46–61. https://doi.org/10.1016/j.tecto.2019.05.011.

Choi, H., Hong, T.-K., He, X., Baag, C.-E., 2012. Seismic evidence for reverse activation of a paleo-rifting system in the East Sea (Sea of Japan). Tectonophysics 572–573, 123–133. https://doi.org/10.1016/j.tecto.2011.12.023.

Clift, P.D., Pecher, I., Kukowski, N., Hampel, A., 2003. Tectonic erosion of the Peruvian forearc, Lima Basin, by subduction and Nazca Ridge collision. Tectonics 22 (3). https://doi.org/10.1029/2002tc001386.
Clift, P., Vannucchi, P., 2004. Controls on tectonic accretion versus erosion in subduction zones: Implications for the origin and recycling of the continental crust. Rev. Geophys. 42 (2), 19–31. https://doi.org/10.1029/2003rg000127.
Dominguez, S., Malavieille, J., Lallemand, S.E., 2000. Deformation of accretionary wedges in response to seamount subduction: Insights from sandbox experiments. Tectonics 19 (1), 182–196. https://doi.org/10.1029/1999tc900055.
Dziewoński, A.M., Chou, T.A., Woodhouse, J.H., 1981. Determination of earthquake source parameters from waveform data for studies of global and regional seismicity. J. Geophys. Res. 86 (B4), 2825–2852. https://doi.org/10.1029/jb086ib04p02825.
Ekström, G., Nettles, M., Dziewoński, A.M., 2012. The global CMT project 2004–2010: Centroid-moment tensors for 13,017 earthquakes. Phys. Earth Planet. In. 200, 1–9. https://doi.org/10.1016/j.pepi.2012.04.002.
Gase, A.C., Bangs, N.L., Saffer, D.M., Han, S., Miller, P.K., Bell, R.E., et al., 2023. Subducting volcaniclastic-rich upper crust supplies fluids for shallow megathrust and slow slip. Sci. Adv. 9 (33), eadh0150. https://doi.org/10.1126/sciadv.adh0150.
Gasperinia, P., Vannuccib, G., 2003. FPSPACK: a package of FORTRAN subroutines to manage earthquake focal mechanism data. Comput. Geosci. 29, 893–901.
He, X., Tao, J., Cao, Y., Pan, F., He, E., Cao, L., Zheng, Y., 2022. No seamount subduction, no magmatic arc? Earth and Planetary Physics 6 (4), 1–6. https://doi.org/10.26464/epp2022031.
Hernández, M.J., Michaud, F., Collot, J.-Y., Proust, J.-N., d'Acremont, E., 2020. Evolution of the Ecuador offshore nonaccretionary-type forearc basin and margin segmentation. Tectonophysics 781, 228374. https://doi.org/10.1016/j.tecto.2020.228374.
Jang, H., Kim, Y., Lim, H., Clayton, R.W., 2019. Seismic attenuation structure of southern Peruvian subduction system. Tectonophysics 771. https://doi.org/10.1016/j.tecto.2019.228203.
Jia, X., Sun, D., 2021. Imaging the crustal interfaces along the Ryukyu arc-trough system using precursors to teleseismic sP and pP. J. Geophys. Res. Solid Earth 126, e2020JB020413.
Kim, Y., Clayton, R.W., 2015. Seismic properties of the Nazca oceanic crust in southern Peruvian subduction system. Earth Planet. Sci. Lett. 429, 110–121. https://doi.org/10.1016/j.epsl.2015.07.055.
Kimura, M., 1985. Back-arc rifting in the Okinawa Trough. Mar. Pet. Geol. 2 (3), 222–240. https://doi.org/10.1016/0264-8172(85)90012-1.
Klein, E., Fleitout, L., Vigny, C., Garaud, J.D., 2016. Afterslip and viscoelastic relaxation model inferred from the large-scale post-seismic deformation following the 2010 M w 8.8 Maule earthquake (Chile). Geophys. J. Int. 205 (3), 1455–1472.
Levitt, D.A., Sandwell, D.T., 1995. Lithospheric bending at subduction zones based on depth soundings and satellite gravity. J. Geophys. Res. Solid Earth 100 (B1), 379–400. https://doi.org/10.1029/94jb02468.
Liu, Z., 2021. When plateau meets subduction zone: A review of numerical models. Earth Sci. Rev. 215. https://doi.org/10.1016/j.earscirev.2021.103556.
Liu, L., Spasojević, S., Gurnis, M., 2008. Reconstructing Farallon Plate Subduction Beneath North America Back to the Late Cretaceous. Science 322 (5903), 934–938. https://doi.org/10.1126/science.1162921.
Ma, L., Chen, L., Cheng, Z., Gerya, T., Li, J., 2022. Bathymetric Highs Control the Along-Strike Variations of the Manila Trench: 2D Numerical Modeling. Front. Earth Sci. 10, 943147. https://doi.org/10.3389/feart.2022.943147.
Margirier, A., Strecker, M.R., Reiners, P.W., Thomson, S.N., Casado, I., George, S.W.M., Alvarado, A., 2023. Late Miocene Exhumation of the Western Cordillera, Ecuador, Driven by Increased Coupling Between the Subducting Carnegie Ridge and the South American Continent. Tectonics 42 (1). https://doi.org/10.1029/2022tc007344.
Mark, H.F., Lizarralde, D., Wiens, D.A., 2023. Constraints on bend-faulting and mantle hydration at the marianas trench from seismic anisotropy. Geophys. Res. Lett. 50 (10). https://doi.org/10.1029/2023gl103331.
Minami, H., Okada, C., Saito, K., Ohara, Y., 2022. Evidence of an active rift zone in the northern Okinawa Trough. Mar. Geol. 443, 106666. https://doi.org/10.1016/j.margeo.2021.106666.
Miyakawa, A., Noda, A., Koge, H., 2022. Evolution of the geological structure and mechanical properties due to the collision of multiple basement topographic highs in a forearc accretionary wedge: insights from numerical simulations. Prog Earth Planet Sci 9 (1), 1. https://doi.org/10.1186/s40645-021-00461-4.
Morgan, J.K., Bangs, N.L., 2017. Recognizing seamount-forearc collisions at accretionary margins: Insights from discrete numerical simulations. Geology 45 (7), 635–638. https://doi.org/10.1130/g38923.1.
Pajang, S., Khatib, M.M., Heyhat, M., Cubas, N., Bessiere, E., Letouzey, J., et al., 2022. The distinct morphologic signature of underplating and seamounts in accretionary prisms, insights from thermomechanical modeling applied to Coastal Iranian Makran. Tectonophysics 845, 229617. https://doi.org/10.1016/j.tecto.2022.229617.
Pan, C., He, X., 2023. Subducting passive continental margins with crustal (ultra)mafic intrusions: An underappreciated mechanism for recycling water back into the mantle. Earth Planetary Phys. 7 (5), 1–6. https://doi.org/10.26464/epp2023074.
Passarelli, L., Cesca, S., Nooshiri, N., Jónsson, S., 2022. Earthquake fingerprint of an incipient subduction of a bathymetric high. Geophys. Res. Lett. https://doi.org/10.1029/2022gl100326.
Pedoja, K., Ortlieb, L., Dumont, J.F., Lamothe, M., Ghaleb, B., Auclair, M., Labrousse, B., 2006. Quaternary coastal uplift along the Talara Arc (Ecuador, Northern Peru) from new marine terrace data. Mar. Geol. 228 (1–4), 73–91. https://doi.org/10.1016/j.margeo.2006.01.004.
Prada, M., Bartolomé, R., Gras, C., Bandy, W.L., Dañobeitia, J.J., 2023. Trench-parallel ridge subduction controls upper-plate structure and shallow megathrust seismogenesis along the Jalisco-Colima margin, Mexico. Commun. Earth Environ. 4 (1), 53. https://doi.org/10.1038/s43247-023-00705-9.
Ruh, J.B., Sallarès, V., Ranero, C.R., Gerya, T., 2016. Crustal deformation dynamics and stress evolution during seamount subduction: High-resolution 3-D numerical modeling. J. Geophys. Res. Solid Earth 121 (9), 6880–6902. https://doi.org/10.1002/2016jb013250.
Sato, T., Koresawa, S., Shiozu, Y., Kusano, F., Uechi, S., Nagaoka, O., Kasahara, J., 1994. Microseismicity of back-arc rifting in the Middle Okinawa Trough. Geophys. Res. Lett. 21 (1), 13–16. https://doi.org/10.1029/93gl02911.
Scholz, C.H., Small, C., 1997. The effect of seamount subduction on seismic coupling. Geology 25 (6), 487–490. https://doi.org/10.1130/0091-7613(1997)025<0487:teosso>2.3.co;2.
Sdrolias, M., Müller, R.D., 2006. Controls on back-arc basin formation. Geochem., Geophys., Geosyst. 7 (4). https://doi.org/10.1029/2005gc001090.
Straub, S.M., Gómez-Tuena, A., Vannucchi, P., 2020. Subduction erosion and arc volcanism. Nat. Rev. Earth Environ. 29, 279. https://doi.org/10.1038/s43017-020-0095-1.
Sun, T., Saffer, D., Ellis, S., 2020. Mechanical and hydrological effects of seamount subduction on megathrust stress and slip. Nat. Geosci. 39 (3), 819. https://doi.org/10.1038/s41561-020-0542-0.
Tao, J., Dai, L., Lou, D., Li, Z.-H., Zhou, S., Liu, Z., et al., 2020. Accretion of oceanic plateaus at continental margins: numerical modeling. Gondwana Res. 81, 390–402. https://doi.org/10.1016/j.gr.2019.11.015.
von Huene, R., Ranero, C.R., Vannucchi, P., 2004. Generic model of subduction erosion. Geology 32 (10), 913–916. https://doi.org/10.1130/g20563.1.
Wang, K., Bilek, S.L., 2011. Do subducting seamounts generate or stop large earthquakes? Geology 39 (9), 819–822. https://doi.org/10.1130/g31856.1.
Wang, K., Bilek, S.L., 2014. Invited review paper: fault creep caused by subduction of rough seafloor relief. Tectonophysics 610, 1–24.
Wang, X., Cao, L., Zhao, M., Cheng, J., He, X., 2022. What conditions promote atypical subduction: insights from the Mussau Trench, the Hjort Trench, and the Gagua Ridge. Gondwana Res. 120, 207–218. https://doi.org/10.1016/j.gr.2022.10.014.
Wang, C., Ding, W., Li, J., Dong, C., Fang, Y., Tang, L., et al., 2019. Effects of trench-perpendicular ridge subduction on accretionary wedge deformation: clues from analogue modelling. Geol. J. 54 (4), 2665–2678. https://doi.org/10.1002/gj.3317.
Wang, C., Ding, W., Schellart, W.P., Li, J., Dong, C., Fang, Y., et al., 2021. Effects of multi-seamount subduction on accretionary wedge deformation: Insights from analogue modelling. J. Geodyn. 145, 101842. https://doi.org/10.1016/j.jog.2021.101842.
Wang, Z., Lin, J., 2022. Role of fluids and seamount subduction in interplate coupling and the mechanism of the 2021 Mw 7.1 Fukushima-Oki earthquake, Japan. Earth Planetary Sci. Lett. 584, 117439. https://doi.org/10.1016/j.epsl.2022.117439.
Wessel, P., Smith, W.H.F., 1991. Free software helps map and display data. Eos 72 (41), 441–446. https://doi.org/10.1029/90EO00319.
Yan, Z., Chen, L., Zuza, A.V., Tang, J., Wan, B., Meng, Q., 2022. The fate of oceanic plateaus: subduction versus accretion. Geophys. J. Int. https://doi.org/10.1093/gji/ggac266.
Yang, J., Zhao, L., Li, Y., 2022. Tectonic deformation at the outer rise of subduction zones. Geophys. J. Int. https://doi.org/10.1093/gji/ggac402.
Zeng, Z., Yu, S., Wang, X., Fu, Y., Yin, X., Zhang, G., et al., 2010. Geochemical and isotopic characteristics of volcanic rocks from the northern East China Sea shelf margin and the Okinawa Trough. Acta Oceanol. Sin. 29 (4), 48–61. https://doi.org/10.1007/s13131-010-0050-y.
Zeumann, S., Hampel, A., 2017. Impact of Cocos Ridge (Central America) subduction on the forearc drainage system. Geology 45 (10), 907–910. https://doi.org/10.1130/g39251.1.
Zhang, J., Zhang, F., Yang, H., Lin, J., Sun, Z., 2021. The effects of plateau subduction on plate bending, stress, and intraplate seismicity. Terra Nova. https://doi.org/10.1111/ter.12570.
Zhao, H., Leng, W., 2023. Aseismic ridge subduction and flat subduction: Insights from three-dimensional numerical models. Earth and Planetary Physics 7 (2), 269–281. https://doi.org/10.26464/epp2023032.
Zhou, Z., Lin, J., Behn, M.D., Olive, J., 2015. Mechanism for normal faulting in the subducting plate at the Mariana Trench. Geophys. Res. Lett. 42 (11), 4309–4317. https://doi.org/10.1002/2015gl063917.